Korean J. Chem. Eng., 33(12), 3367-3373 (2016)
DOI: 10.1007/s11814-016-0191-6

pISSN: 0256-1115
eISSN: 1975-7220

Nanopillars TiO_2 thin film photocatalyst application in the remediation of aquatic environment

C. Lalhriatpuia*, Alka Tiwari, Alok Shukla**, Diwakar Tiwari***, and Seung Mok Lee****,†**

*Department of Chemistry, Pachhunga University College, Aizawl 796001, India
**Department of Physics, National Institute of Technology, Aizawl 796001, India
***Department of Chemistry, School of Physical Sciences, Mizoram University, Aizawl 796004, India
****Department of Health and Environment, Catholic Kwandong University, 522 Naegok-dong, Gangneung 25601, Korea
(*Received 9 April 2016 • accepted 30 June 2016*)

Abstract−We assessed the photocatalytic behavior of Nanopillars-TiO_2 thin films obtained onto a borosilicate glass in the degradation of 17α-ethynylestradiol (EE2) from aqueous solution under batch reactor operations. The thin films were characterized by the XRD, SEM, AFM analytical methods. BET specific surface area and pore sizes were also obtained. The photocatalytic degradation of EE2 using the UV light was studied at wide range of physico-chemical parametric studies to determine the mechanism of degradation as well the practical implacability of the technique. The batch reactor operations were conducted at varied pH (pH 4.0 to 10.0), EE2 initial concentration (1.0 to 5.0 mg/L) and presence of several interfering ions, i.e., cadmium nitrate, copper sulfate, zinc chloride, sodium chloride, sodium nitrate, sodium nitrite, glycine, oxalic acid and EDTA in the photocatalytic degradation of EE2. The time dependence photocatalytic degradation of EE2 was demonstrated with the pseudo-first-order rate kinetics. The mineralization of EE2 was assessed using the total organic carbon analysis conducted at varied initial pH and EE2 concentrations. Further, the repeated use of the photocatalyst enhanced the applicability of thin films in the successive photocatalytic operations.

Keywords: Immobilized Nanopillar-TiO_2, Thin Films, 17α-Ethynylestradiol, Photocatalyst, Mineralization, Kinetics

INTRODUCTION

The enhanced use of steroidal hormones has received greater attention due to its high persistency, low biodegradability, high estrogenic property and toxic effects even at low levels. Therefore, these are classified as endocrine disrupting chemicals (EDCs) [1,2]. Their adverse effects in sexual development of animal and decrease in the average number of human spermatozoa is widely reported elsewhere [3]. The estrogenic hormones enter into the aquatic environment through direct runoff, hospital effluents and excretion of un-metabolized drugs or active metabolites [1,4].

17α-Ethynylestradiol or 19-nor-17α-pregna-1,3,5(10)-trien-20-yne-3,17-diol, (*Cf* Structure 1) also known as EE2 is a synthetic steroid estrogen compound widely used in oral contraceptive pills and hormone replacement therapy for the treatment of osteoporosis, menstrual disorders, prostate and breast cancer, and other ailments [5]. This improves livestock productivity and develops single-sex populations of fish to optimize the growth in aquaculture [1,6,7]. EE2, as low as 0.1 ng/L concentration, can induce the synthesis of yolk-precursor protein vitellogenin in male rainbow trout [3]. Exposure to oral micro-molar doses of EE2 can permanently disrupt the reproductive tract of male rats [8]. The normal sewage treatment plants are unable to eliminate EE2 completely, which results in the presence of residual load of pollutants in the effluent water [9].

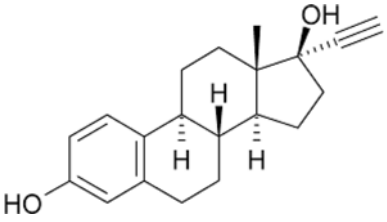

Structure 1. 17α-Ethynylestradiol (EE2).

Therefore, there is a greater attention to effective and efficient remediation of aquatic environment contaminated with estrogenic hormones. Heterogeneous photocatalytic treatment technology utilizing semiconductor titanium dioxide (TiO_2) particles appears to be a promising approach for efficient and environment friendly treatment process for various wastewater treatment strategies. The photo-generated electron-hole pairs (e^-/h^+) enable oxidation and reduction of pollutants adsorbed onto the surface of TiO_2. The e^- and h^+ pairs leads to the formation of radical species, i.e., superoxide radical ($O_2^{\bullet-}$) and hydroxyl radical (•OH), respectively. The redox potential of •OH radical is found seemingly high (E^0=2.80 V), which enables it in efficient oxidation of even stable organic compounds/species from aqueous solutions [10,11]. Literature reveals that UV-C light was employed in the treatment of wastewater obtained from the contraceptive pill manufacturing plant and contained with the EE2 and levonorgestrel (LNG). The photocatalytic removal efficiencies of EE2 and LNG were found to be 92% and

†To whom correspondence should be addressed.
E-mail: leesm@cku.ac.kr

97%, respectively, and suggested that the •OH radical was the main contributor to degrade these pollutants from aqueous solutions [12]. Similarly, DegussaP25 photocatalyst was employed in the photocatalytic degradation of multicomponent system contained with several estrogens, estrone (E1), 17β-estradiol (E2), 17α-ethynyl-estradiol (EE2) and estriol (E3), using UVA and UVC radiations. The quantum yields (moles of estrogens degraded per Einstein of photons absorbed) were estimated and found to be 2.1×10^{-3} to 3.9×10^{-3} under UVC-TiO_2, whereas under UVA-TiO_2 photocatalysis were 1.2×10^{-3} to 1.8×10^{-3} [13]. Catalytic oxidation of EE2 was assessed using the catalyst tetra-amido macrocyclic ligand (Fe^{III}-TAML) complex in presence of hydrogen peroxide. The maximum degradation of EE2 occurred at pH 10.21 with an apparent half-life of 2.1 min, and the oxidized products showed 30% estrogenicity removal as assessed with yeast estrogen screen (YES) bioassay [14]. A newer TiO_2 doped low silica X-zeolite was assessed in the degradation of EE2 using the UV radiations. The catalyst was found to be efficient and the proposed mechanism revealed that the •OH radicals were mainly involved in the degradation of EE2 [15]. A simple photooxidation (λ>290 nm) of 17β-estradiol (E2) and 17α-ethinylestradiol (EE2) was carried out and some of the degradation products were identified [16]. Other study showed a simultaneous photocatalytic treatment of hexavalent chromium (Cr(VI)) and EDCs, i.e., bisphenol A (BPA), 17α-ethinyl estradiol (EE2) and 17β-estradiol (E2), using rotating reactor under solar irradiation and TiO_2 Nanotubes [17].

Although, it was observed that the use of nano-particles or nano-composite TiO_2 photocatalysts was efficient in several wastewater treatment strategies, in particular the degradation of several water pollutants, however; it showed difficulty in effective phase separation of catalyst at the end of unit operation, hence restricting the successive application of catalyst in multiple operations. Moreover, the reactivity of photo-catalyst is greatly hampered with the shadowing effect of nano-particles [15]. Therefore, the TiO_2 Nano-pillar thin films were immobilized onto the glass substrate using the sol-gel template synthesis employing PEG as filler media. The materials were characterized and further employed in the photocatalytic degradation of diclofenac sodium and tetracycline hydrochloride [18] or Aizarin Yellow [19] from aqueous solutions. The present communication is further implication of thin films in the photocatalytic degradation of 17α-Ethynylestradiol (EE2) from aqueous solutions. Various physico-chemical parametric studies were conducted to demonstrate photocatalytic mechanism of EE2 degradation from aqueous solutions. The successive operations of the photocatalyst thin films further demonstrate the applicability of catalyst for its wider industrial implications.

MATERIALS AND METHODS

1. Chemical and Materials

Titanium(IV) isopropoxide, poly(ethylene glycol), 17α-ethynyl-estradiol ($C_{20}H_{24}O_2$), were procured from Sigma Aldrich. Co., USA. Acetylacetone, ethanol anhydrous, hydrochloric acid, sodium hydroxide, zinc chloride, cupric sulfate pentahydrate, cadmium nitrate tetrahydrate, ethylenediaminetetraacetic acid, sodium nitrate, sodium nitrite, oxalic acid, glacial acetic acid were obtained from Merck India Ltd., India. Sodium chloride and glycine were obtained from HiMedia, India Ltd., India. Purified water (18.2 MΩ·cm at 25 °C) was obtained from Millipore Water Purification system (Model: Elix 3) and used for entire solution preparations and other analytical studies.

The HPLC Instrument (Model: Waters 515 HPLC pump, Detector: Waters 2489 UV/Visible Detector, Column: Symmetry ® C18 5 μm (4.6×250 mm column)) was used for the quantitative determination of EE2 using acetonitrile (70%)+water (29%)+glacial acetic acid (1%) by v/v as mobile phase and the absorbance intensity was measured at 276 nm. The total organic carbon content was obtained with a TOC Analyzer (Shimadzu, Japan; Model: TOC-VCPH/CPN).

2. Methodology

2-1. Preparation of Nano-pillars TiO_2 Thin Films

Two types of nano-pillars TiO_2 thin films were obtained without and with filler media (PEG) by the sol-gel synthetic process using Titanium isopropoxide as a precursor. The detailed preparation process was described elsewhere [18,19] and also described briefly here.

2-2. Photo-catalytic Degradation Studies

Photo-catalytic experiments were conducted under batch reactor operations. The reactor consisted of a black box (dimension: 60×45×45 cm). A 100 mL borosilicate glass beaker containing 50 mL of pollutant solution was placed inside the reactor and a thin film (prepared without PEG (S1)) or (prepared with PEG (S2)) was placed horizontally at the bottom of the reactor. A UV-C lamp having maximum wavelength, λ=253.7 nm (Model: Phillips TUV 11W, 4 P.SE; Poland) was placed at the top of the reactor (i.e., 10 cm above the solution). The UV-radiation was used to reach the TiO_2 photocatalyst through the pollutant solution, causing the photocatalytic oxidation at the catalyst surface. The reaction temperature was maintained at 25±1 °C using the self-assembled water-bath. Air was bubbled to the pollutant solution with an aquarium air pump. The final pollutant concentration after 4 h irradiation was determined employing the HPLC. Always, a blank experiment was performed under UV irradiation only using no thin film photocatalyst for comparison.

Stock solution of EE2 (10.0 mg/L) was prepared in purified water. The required experimental EE2 concentration was obtained by the successive dilution of stock solution. The pH of these solutions was maintained adding drop-wise conc. HCl/NaOH solutions. The concentration dependence data was obtained varying the EE2 concentrations from 1.0 to 5.0 mg/L. The degradation efficiency of EE2 was calculated by using Eq. (1):

$$\text{Removal Efficiency} = \frac{C_i - C_f}{C_i} \times 100 \quad (1)$$

where C_i and C_f are the concentrations of EE2 before and after the photocatalytic treatment.

2-3. Characterization of Thin Films

The X-ray diffraction (XRD) pattern of the thin films S1 and S2 samples was collected using X-ray diffraction machine, i.e., PANalytical, Netherlands (Model X'Pert PRO MPD) with a scan rate of 0.034 of 2θ illumination at an applied voltage of 45 kV and a measured current 35 mA. The Cu K_α radiation was employed having

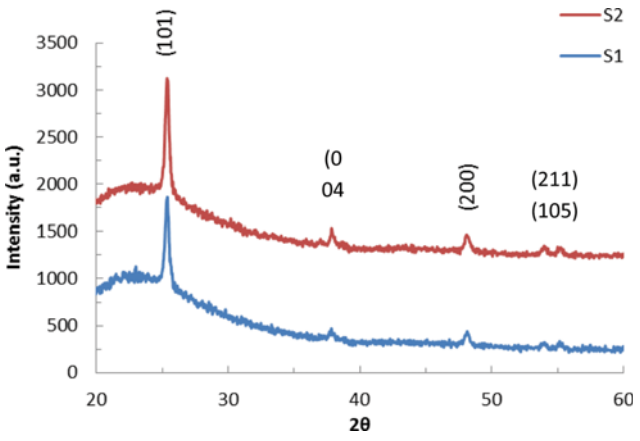

Fig. 1. X-ray diffraction pattern for the S1 and S2 thin films.

wavelength of 1.5418 Å. Surface morphology was observed by scanning electron microscopy (FE-SEM SU-70, Hitachi, Japan) and atomic force microscopy. AFM measurements were carried in the non-contact mode, using XE-100 apparatus from Park Systems (2011) having sharp tips (>8 nm tip radius; PPP-NCHR type from Nanosensors™). The topographical 3D AFM images were taken over the area of 10×10 μm^2. Moreover, the BET specific area was obtained using Protech Korea BET surface area analyzer (Model ASAP 2020).

RESULTS AND DISCUSSION

1. Characterization of Thin Films

XRD pattern obtained for the S1 and S2 samples is shown in Fig. 1 and elsewhere [18]. The characteristic peaks obtained at the 2θ values of 25.39, 37.84, 48.14, 53.44 and 54.59 (for S1 samples) were assigned to the TiO_2 anatase phase [18,19]. Almost an identical XRD pattern was obtained for the S2 sample. The size of particles for S1 and S2 catalysts calculated by Scherer's formula [18] was found to be 25.4 and 21.9 nm, respectively. This further suggests that the S1 and S2 were comprised with nano-sized, perhaps the nano-pillars TiO_2 which were evenly distributed on the substrate surface.

Fig. 2 shows the SEM images of these two samples, S1 and S2, also presently previously [19]. It was observed that the S1 sample had nano-sized pillars of TiO_2. The average size of these pillars was less than 15 nm, which are very evenly distributed and forming a thin film onto the substrate surface. However, the S2 thin films were found more disordered, possessing several cracks onto the surface. The BET pore size was in the order of 4-8 nm and the Scherrer diameter was calculated to 21-29 nm. Also, a regular network was obtained onto the substrate surface and, possibly, the titania was forming nano-pillars onto the substrate with an average size of ~30 nm.

The 3D AFM images of S1 and S2 samples are shown in Fig. 3 were also presented elsewhere [18]. A homogeneous distribution

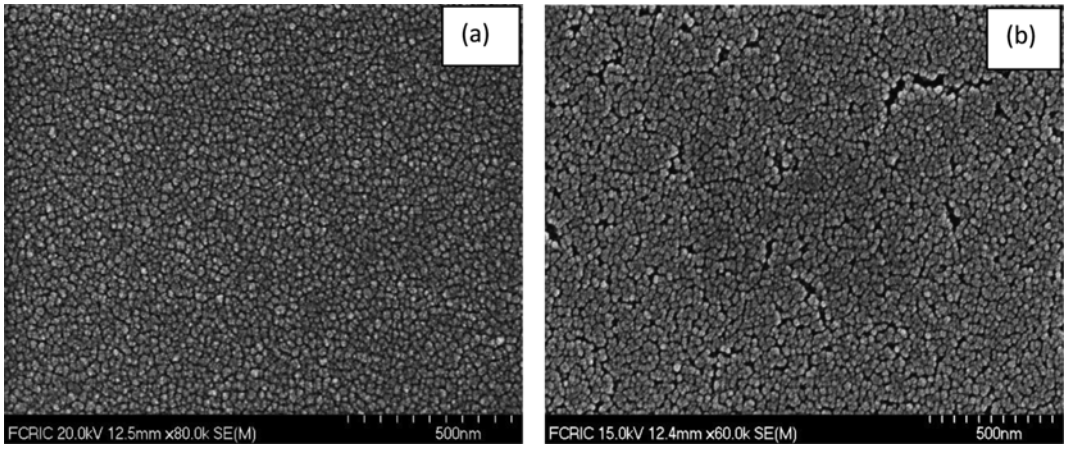

Fig. 2. FE-SEM images of thin films (a) S1, and (b) S2 [19].

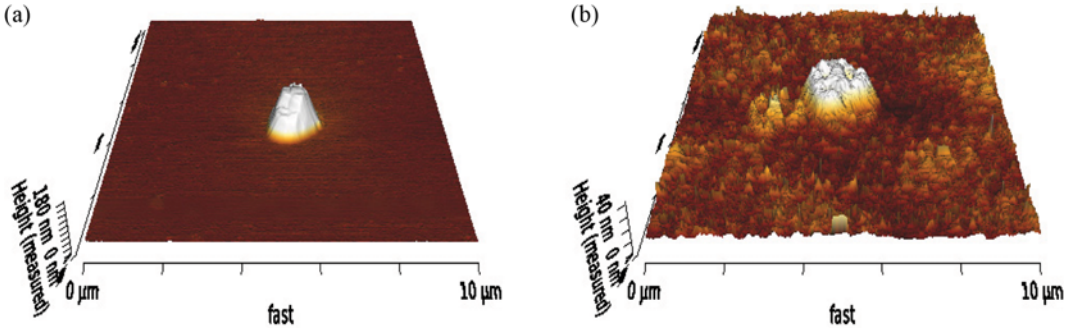

Fig. 3. 3D AFM images of S1 and S2 samples at the scale of 10×10 μm^2 [18].

Table 1. BET specific surface area and pore sizes obtained for S1 and S2 samples

Solid materials	BET specific surface area (m^2/g)	Pore sizes (nm)
S1	5.217	7.77
S2	1.420	4.16

of TiO_2 Nano-pillars, indicating optically smooth films, was obtained with S1. However, a non-uniform distribution of particles was observed with the S2 thin film. Further, the average height of the pillars was found to be 180 nm and 40 nm, respectively, for the S1 and S2 samples. These results were in good agreement with the above SEM observation. Moreover, the calculated average roughness (Ra) and root mean square roughness (Rq) parameters for S1 and S2 samples were 3.523, 14.06 nm and 2.708, 4.668 nm, respectively.

The BET specific surface area and pore sizes of S1 and S2 catalyst are shown in Table 1 also reported previously [19]. Although the specific surface area of the catalyst was decreased with the thin film in presence of PEG, however the mesopore size decreased significantly. This enhanced the possibility of the pollutants to trap within the pores and could show an enhanced catalytic activity.

2. Photocatalytic Degradation of EE2

2-1. Effect of pH in the Degradation of EE2

The effect of pH is an important parameter in the degradation/oxidation of pollutants since it deals with the mechanism involved on the surface of photocatalyst. The catalytic action was greatly influenced with the sorption of pollutants on the catalyst surface and sorption was highly dependent to the solution pH. Therefore, the effect of pH in the degradation of EE2 was conducted over a wide pH range, pH 4.0 to 10.0, at a constant EE2 initial concentration (2.0 mg/L). The pH dependence degradation of EE2 is presented in Fig. 4. Fig. 4 clearly indicates that the percentage of EE2 removal was increased up until pH 6.0, beyond which it started slightly to decrease up to pH 10.0. This suggests that an optimum pH 6.0 could be an appropriate pH for better performance of photocatalyst. The extent of degradation was affected by the surface charge properties of S1 and S2 as well the speciation of the EE2 molecule at varied solution pH values. It was assumed that TiO_2 surface remained positively charged in the acidic media (pH<6.9) and negatively charged in alkaline solutions (pH>6.9) as the point of zero charge for S1 and S2 was obtained to 6.9. On the other hand, the EE2 molecule remained at its molecular form at pH<10.5 as the pK_a value of EE2 was reported to be 10.5 [20]. The low degradation observed at acidic condition (i.e., pH 4.0) was due the fact that in the presence of dissolved oxygen, water molecules generate •OH, hydrated electrons (e^-_{aqua}), and •H under UV irradiation according to the equation [21,22]:

$$H_2O+hv \rightarrow e^-_{aqua}+\bullet H+\bullet OH+H^+ \quad (2)$$

Therefore, the formation of •OH is greatly suppressed in acidic media as shown in Eq. (2). Moreover, excess of H^+ ion scavenged the hydroxyl radical (•OH), thus causing to decrease EE2 degradation. Thus, with increase in pH at pH 6.0, the catalyst surface showed an enhanced affinity towards the pollutants; thereby, an increased in degradation reaction was observed. However, further increase in pH up to pH10.0, the EE2 molecule was dissociated (i.e., the conjugated base) losing the protons to the hydroxide ions [23]. As a result, an electrostatic repulsion occurred between the negatively charge catalyst surface and anionic charge of the pollutant, which ultimately affected the degradation of EE2 to some extent. Moreover, a separate study showed that various modified clay hybrid materials possessed relatively high sorption capacity within the pH region 5-8 where EE2 was strongly sorbed onto the solid surface [5].

2-2. Effect of EE2 Concentration

The effect of pollutant concentration was studied at varied EE2 concentrations, 1.0 to 5.0 mg/L at pH 6.0. The final concentration after 4 h irradiation was obtained using the HPLC measurements and the results were computed as percent removal of EE2 as a function of initial EE2 concentration and returned in Fig. 5. The percent degradation of EE2 was increased from 62.11 to 78.01% (by S2 sample); from 39.59 to 56.03% (by S1 sample) and from 20.21 to 33.38% (by UV only) decreasing the EE2 concentration

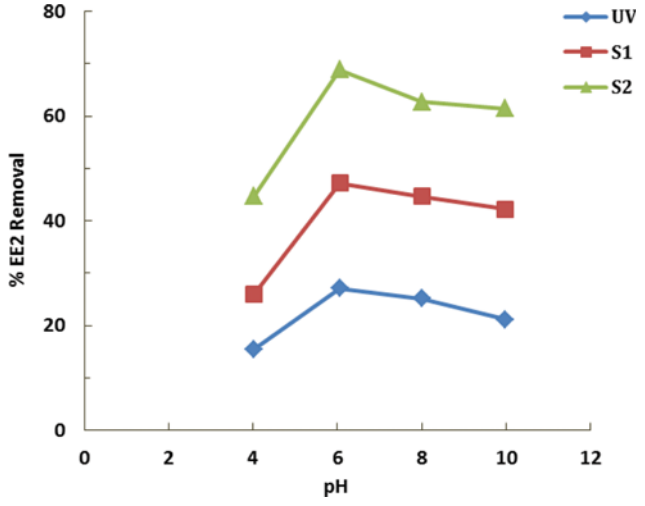

Fig. 4. Effect of pH in the photocatalytic degradation of EE2 using UV, S1 and S2.

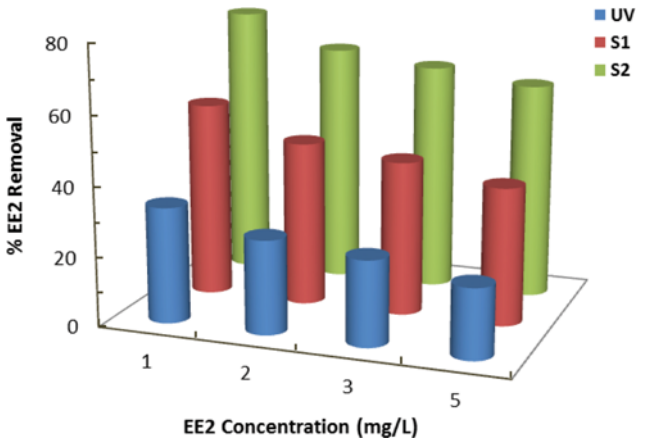

Fig. 5. Effect of concentration in the photocatalytic degradation of EE2 using thin films.

from 5.0 to 1.0 mg/L, respectively. These results further indicated that the thin films S1 and S2 showed significantly higher photocatalytic activity in the efficient degradation of EE2 from aqueous solutions compared to the UV only irradiated samples. Furthermore, the PEG template thin film S2 sample had more enhanced photocatalytic activity than the S1 samples, since more EE2 molecules were effectively trapped inside the small mesopores provided by the catalyst surface, and hence, effectively oxidized by the reactive species. The increase in EE2 concentration restricts the penetration of UV light into the pollutant solution, which introduced an inner filter effect and the solution became more impermeable for UV-radiations, which therefore limited the generation of active hydroxyl radicals and restricted the photocatalytic activity [24]. It was previously reported that the increasing the EE2 concentration was caused for significant decrease in the EE2 removal in a UV/H_2O_2 treatment system [20].

2-3. Photocatalytic Degradation Kinetics of EE2

The photo-catalytic degradation kinetics of EE2 was studied using the change in C_t/C_0 values (where C_0 is the initial concentration of EE2 and C_t is the concentration of EE2 at time 't') as a function of time and results are presented graphically in Fig. 6. The figure clearly indicates that a sharp decrease in degradation of EE2 was observed in presence of thin films S1 and S2 after the 4 h UV irradiation. At the end of 4 hrs irradiation the C_t/C_0 values were found to be 0.31, 0.53 and 0.73 for the S2, S1 and photolysis only, respectively. A significant lower value of C_t/C_0 was obtained using the S2 sample compared to the S1 sample. This again confirmed the affinity of the pollutant towards the thin film (S2) surface and enhanced photo-catalytic degradation of EE2 at the surface occurred.

The kinetics of the EE2 degradation was represented using the known pseudo-first-order rate equation (Eq. (3)):

$$r = -\frac{d[EE2]}{dt} = k_{app}[K_{photolysis} + k_{photocatalysis}][EE2] = k_{app}[EE2] \quad (3)$$

where [EE2] represents the concentration of estrogen and k_{app} is the pseudo-first-order rate constant. It is obvious that the k_{app} depends on the concentration of EE2.

Integration of Eq. (3) with the extreme conditions, i.e., at t=0 the [EE2]=C_o. Eq. (3) resulted in Eq. (4):

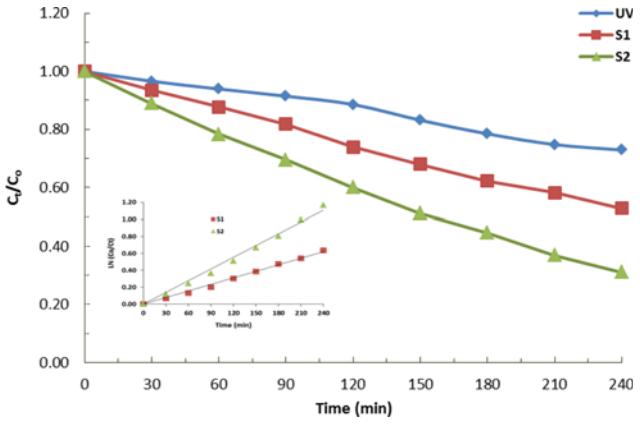

Fig. 6. Kinetics of photocatalytic degradation of EE2 using thin films.

Table 2. Kinetic data obtained in the photocatalytic degradation of EE2 using various photocatalysts

Samples	Pseudo- first order rate constant ($k_{app}\times10^{-3}$)/min	R^2
UV only	1.3	0.975
S1	2.6	0.995
S2	4.6	0.991
T1	3.7	0.999
T2	5.5	0.997

$$LN\left(\frac{C_o}{C_t}\right) = k_{app} \cdot t \quad (4)$$

Straight lines were drawn between the LN (C_o/C_t) against time 't'. The results obtained are presented graphically in Fig. 6 (inset) for the EE2 photocatalytic degradation (Initial concentration of EE2: 2.0 mg/L and at pH: 6.0). The pseudo-first-order rate constants (k_{app}) and R^2 values were obtained for S2, S1 and photolysis treatment and returned in Table 1. It is clear from kinetic fitting that the photo-degradation of EE2 reasonably fitted well to the pseudo-first-order rate kinetics using the thin films. Kinetic results were also obtained using the powder T1 and T2 samples in the degradation of EE2 ([EE2]: 2.0 mg/L at pH 6.0 and dose of solid: 0.1 g/L) and given in Table 2. Results indicated that the apparent rate constant of EE2 degradation by the respective S1 and S2 samples was almost comparable with its powder samples T1 and T2. Previously, it was reported that the azo dye methyl orange followed first-order rate kinetics using the TiO_2 and Ag deposited TiO_2. The Ag deposited TiO_2 showed an enhanced catalytic action with apparent pseudo-first-order rate constant of 7.765×10^{-2}, whereas TIO_2 was 4.521×10^{-2} min^{-1} in the degradation of methyl red [25]. Similarly, the UVC/TiO_2 system showed pseudo-first-order rate kinetics in the simultaneous degradation of EE2 and LNG from different matrix and ranging from 2.2×10^{-2} to 10.8×10^{-2} min^{-1} [12].

2-4. Mineralization of EE2

The mineralization of EE2 was studied varying the pollutant concentration from 1.0 to 5.0 mg/L at constant pH 6.0 employing S1 and S2 photocatalyst along with the photolysis only. Results were obtained at the end of 4 h of photo-irradiation. Percent of TOC removal as a function of EE2 concentration is presented graphically in Fig. 7(a). The results implied that increasing the concentration of EE2, a sharp decrease in TOC was observed. Quantitatively, increasing the concentration of EE2 from 1.0 to 5.0 mg/L the percent of TOC was decreased from 26.35 to 11.60% (using S2 thin films); 19.99 to 6.97% (using S1thin films) and 18.82 to 9.36% (using UV only). However, prolonged irradiation, 24 h, using S2 photocatalyst enabled to increase the TOC removal even up to 61.58%. These results indicated that even a partial mineralization of EE2 was achieved using the thin films; however, prolonged treatment may provide a complete mineralization of EE2 from aqueous solutions. The low percent TOC removal rendered relatively a higher stability of the EE2 molecule with large aromatic ring structure as well as the intermediates formed after partial degradation in the photocatalytic reaction. The hydroxyl radicals •OH are highly reactive and readily mineralizing the EE2. This may even

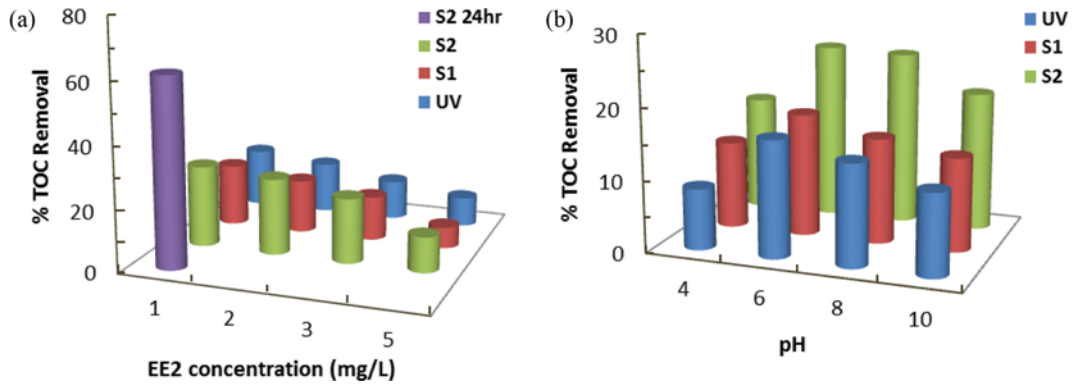

Fig. 7. Percent TOC removal of EE2 as a function of (a) EE2 concentration, (b) pH, in the photo-catalytic degradation using thin films.

break the C-C, C=C, C≡C or C=O and O-H bonds in aqueous solution of EE2, resulting in the formation of CO_2 and other inorganic ions [26,27]. It was reported that the holes may directly decompose the EE2 onto the catalyst surface [15], which ultimately causes enhanced mineralization of EE2 at prolonged duration of irradiation.

Again, the percent TOC removal as a function of pH was studied in order to optimize the best possible pH of EE2 degradation and to achieve a maximum mineralization of the EE2 in the photocatalytic treatment. The EE2 solution ([EE2]: 2.0 mg/L) was treated at different pH values (pH 4.0 to 10.00) for 4 h using the UV only, S1 and S2 samples and the percent of TOC removal was presented as a function of pH in Fig. 7(b). These results were again in agreement with the pH dependence removal of EE2 in the photocatalytic degradation.

2-5. Effect of Interfering Ions

To simulate the natural waste water matrix, we assessed the applicability of thin film (S2) in the photocatalytic degradation of EE2 in presence of several interfering ions (10.0 mgL^{-1}): cadmium nitrate, copper sulfate, zinc chloride, sodium chloride, sodium nitrate, sodium nitrite, glycine, oxalic acid and EDTA. The samples were irradiated for 4 h at pH 6.0, and the initial concentration of EE2 was kept constant at 2.0 mg/L. The percent removal of EE2 was presented as a function of interfering ions and returned in Fig. 8. It was observed that the degradation of EE2 was hampered to a varied extent in the presence of different interfering ions. The inhibition caused by the co-existing ions in the reaction medium was mainly due to the scavenger properties of the cations or anions, as the photocatalytic degradation processes were predominantly driven by the highly oxidizing species, photogenerated valence band holes (h^+) or hydroxyl radicals (•OH). Previously, it was also stated that the removal efficiency of EE2 depended largely on the hydroxyl radicals and the presence of other organic species may compete for the hydroxyl radicals and hence show a reduce photocatalytic efficiency for the EE2 [28].

2-6. Reusability of Thin Films in Repeated Operations

Further, the applicability of thin films was assessed for its reusability in repeated operations. The reusability test was performed using the two thin films S1 and S2 in the degradation of EE2 at a fixed initial EE2 concentration (2.0 mg/L) at pH 6.0 for 2 h irradiation, and experiments were repeated for the five consecutive experimental runs. The percent removal of EE2 was computed at the end of each cycle and results presented graphically in Fig. 9. The results showed insignificant decrease in percent degradation of EE2 even at the end of five experimental runs using S1 or S2

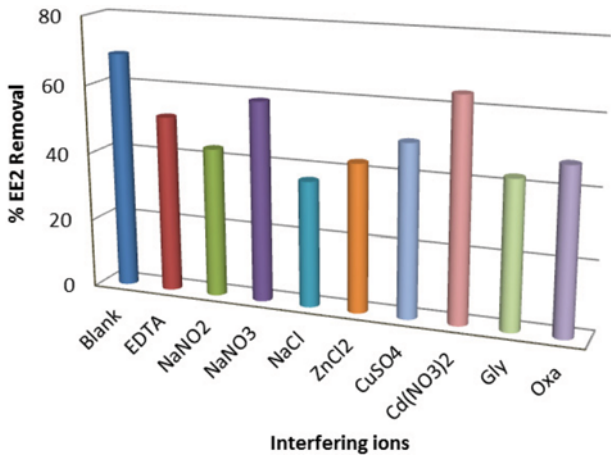

Fig. 8. Photocatalytic degradation of EE2 in presence of interfering ions using S2 thin film.

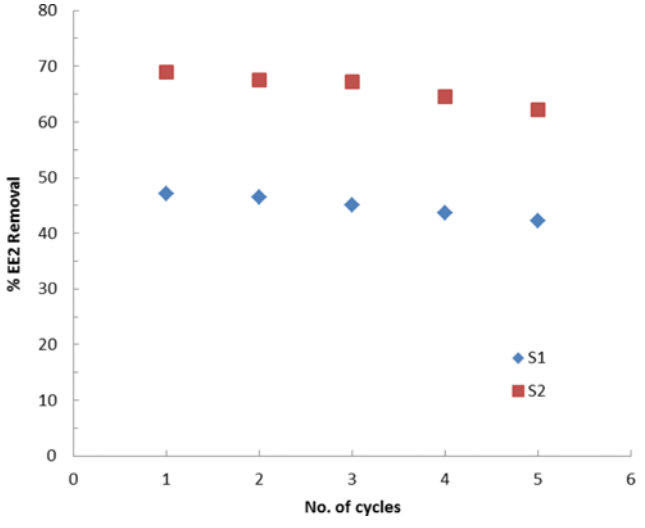

Fig. 9. Percent degradation of EE2 using S1 and S2 thin films with respect to repetitive operations.

samples. More quantitatively, the reduction in catalytic activity of these thin films was found to be 4.88% (using S1) and 6.75% (using S2) for the degradation of EE2 obtained at the end of five cycles of photocatalytic operations. These results indicated that the thin film S1 and S2 could be reused without much decline in photocatalytic activity of the catalyst. This apparently overcomes the problem of separation of catalyst from the slurry or even may provide the cost effectiveness of the overall process. Furthermore, this could enhance the practical implacability of the catalyst in industrial applications we well.

CONCLUSIONS

The TiO_2-Nanopillars photocatalysts were immobilized onto the borosilicate glass. The sol-gel synthetic route was adopted for thin film preparation with (S1) and without (S2) PEG (polyethylene glycol) as filler media. XRD data revealed that anatase phase of TiO_2 was immobilized onto the glass substrate. Surface morphology obtained with the SEM images of these solids showed fine grains of TiO_2 were very evenly distributed onto the substrate and forming a thin layer of TiO_2 particles for S1 sample. Whereas S2 showed relatively disordered surface structure and the film possessed several micro-cracks on the surface. The SEM images further indicated the particulates' average size was *Ca* 15 nm. AFM analytical data showed that the TiO_2 had a mean pillar size of 180 and 40 nm for the S1 and S2 samples, respectively. Moreover, the average roughness (Ra) and root mean square roughness (Rq) were 3.523, 14.06 nm and 2.708, 4.668 nm, respectively, for S1 and S2 samples. Similarly, BET surface area was 5.217 and 1.420 m^2/g, with the pore size 7.77 and 4.16 nm, respectively, for the S1 and S2 thin films. Furthermore, catalysts were employed in the photocatalytic degradation of potential endocrine disruptor EE2 from aqueous solutions. Relatively, very high degradation occurred at pH 6.0, which was slightly decreased at higher pH conditions. Decreasing the EE2 initial concentration favored greatly the efficiency of photocatalyst in the percent degradation of EE2. Similarly, the mineralization of this estrogen increased with decreasing the pollutant concentration. The degradation process followed pseudo-first-order rate kinetics. The presence of several cations and anions affected to some extent the photo-catalytic degradation of EE2 using the S2 photocatalyst. Overall the S1 and S2 thin films showed very high percent degradation of EE2 compared to the photolysis. S2 showed relatively higher photocatalytic efficiency compared to the S1 photocatalyst. The repetitive use of thin film catalysts showed insignificant decrease in the percent degradation of EE2 from aqueous solutions enabled the S1 and S2 thin films to be potential and cost-effective photocatalysts which could possess greater practical or industrial applicability.

ACKNOWLEDGEMENT

One of the authors C. Lalhriatpuia wishes to acknowledge UGC-NERO for the financial support as in the form of Minor Research Project (vide No.: F.5-93/2014-15/MRP/NERO).

REFERENCES

1. V. Belgiorno, L. Rizzo, D. Fatta, C. D. Rocca and G. Lofrano, *Desalination*, **215**, 166 (2007).
2. R. Xia, Z. Li , B. Cheng and K. Su, *Korean J. Chem. Eng.*, **31**, 427 (2014).
3. X. Zhang, P. Chen, F. Wu, N. Deng, J. Liu and T. Fang, *J. Hazard. Mater. B*, **133**, 291 (2006).
4. G. G. Ying, R. S. Kookana and Y. J. Ru, *Environ. Int.*, **28**, 545 (2002).
5. Thanhmingliana, S. M. Lee, D. Tiwari and S. K. Prasad, *RSC Adv.*, **5**, 46834 (2015).
6. J. Han, W. Qiu, Z. Cao, J. Hu and W. Gao, *Water Res.*, **47**, 2273 (2013).
7. J. de Rudder, T. V. de Wiele, W. Dhooge, F. Comhaire and W. Verstraete, *Water Res.*, **38**, 184 (2004).
8. S. Larcher, G. Delbès, B. Robaire and V. Yargeau, *Environ. Int.*, **39**, 66 (2012).
9. S. Larcher and V. Yargeau, *Environ. Pollut.*, **173**, 17 (2013).
10. M. M. Haque and M. Muneer, *Dyes Pigm.*, **75**, 443 (2007).
11. K. Natarajan, P. Singh, H. C. Bajaj and R. J. Tayade, *Korean J. Chem. Eng.*, **33**, 1788 (2016).
12. D. Nasuhoglu, D. Berk and V. Yargeau, *Chem. Eng. J.*, **185-186**, 52 (2012).
13. G. J. Puma, V. Puddu, H. K. Tsang, A. Gora and B. Toepfer, *Appl. Cat. B: Environ.*, **99**, 388 (2010).
14. J. L. Chen, S. Ravindran, S. Swift, L. J. Wright and N. Singhal, *Water Res.*, **46**, 6309 (2012).
15. Z. Pan, E. A. Stemmler, H. J. Cho, W. Fan, L. A. LeBlanc, H. H. Patterson and A. Amirbahman, *J. Hazard. Mater.*, **279**, 17 (2014).
16. P. Mazellier, L. Méité and J. D. Laat, *Chemosphere*, **73**, 1216 (2008).
17. Y. Kim, H. Joo, N. Her, Y. Yoon, J. Sohn, S. Kim and J. Yoon, *J. Hazard. Mater.*, **288**, 124 (2015).
18. C. Lalhriatpuia, D. Tiwari, A. Tiwari and S. M. Lee, *Chem. Eng. J.*, **281**, 782 (2015).
19. D. Tiwari, C. Lalhriatpuia, Lalhmunsiama, S. M. Lee and S. H. Kong, *Appl. Surf. Sci.*, **353**, 275 (2015).
20. Z. Zhang, Y. Feng, Y. Liu, Q. Sun, P. Gao and N. Ren, *J. Hazard. Mater.*, **181**, 1127 (2010).
21. A. Zhang, Y. Li, *Sci. Total Environ.*, **493**, 307 (2014).
22. Y. Kwon and H. Lee, *Korean J. Chem. Eng.*, **32**, 2429 (2015).
23. S. B. Fredj, J. Nobbs, C. Tizaoui and L. Monser, *Chem. Eng. J.*, **262**, 417 (2015).
24. N. Daneshvar, M. A. Behnajady, M. K. A. Mohammadi and M. S. S. Dorraji, *Desalination*, **230**, 16 (2008).
25. L. G. Devi and K. M. Reddy, *Appl. Surf. Sci.*, **256**, 3116 (2010).
26. S. Fukahori, H. Ichiura, T. Kitaoka and H. Tanaka, *Appl. Catal. B: Environ.*, **46**, 453 (2003).
27. M. V. Shankar, S. Anandan, N. Venkatachalam, B. Arabindoo and V. Murugesan, *Chemosphere*, **63**, 1014 (2006).
28. T. Karpova, S. Preis and J. Kallas, *Int. J. Photoenergy*, **2007**, 1 (2007).